

FROM BILLIARDS TO THERMODYNAMIC LAWS: I. STOCHASTIC ENERGY EXCHANGE MODEL

YAO LI AND LINGCHEN BU

ABSTRACT. This paper studies a billiards-like microscopic heat conduction model, which describes the dynamics of gas molecules in a long tube with thermalized boundary. We numerically investigate the law of energy exchange between adjacent cells. A stochastic energy exchange model that preserves these properties is then derived. We further numerically justified that the stochastic energy exchange model preserves the ergodicity and the thermal conductivity of its deterministic counterpart.

1. INTRODUCTION

The derivation of macroscopic thermodynamic laws from microscopic Hamiltonian dynamics is a century-old challenge since the time of Boltzmann. When a system is out of equilibrium, it is very difficult to prove that deterministic interactions among gas molecules or crystal structures leads to Fourier's law [1]. From a dynamical systems point of view, deterministic interactions of gas molecules can be modeled as elastic collisions of particles. However, many-particle billiards is a well known challenge, with only very few known result [3, 27, 28].

On the other hand, there are also stochastic microscopic heat conduction models which assumes some randomness among particle interactions or energy transports. Stochastic models are known to be more tractable. There have been numerous known results about the nonequilibrium steady-state, entropy production rate, fluctuation theorem, thermal conductivity, and Fourier's law for various stochastic models [10, 14, 17, 24, 8, 9, 25, 26]. Therefore, it is tempting to reduce a deterministic heat conduction model to a stochastic one. One example is [22], in which a particle-disk collision model is well-approximated by a stochastic particle system.

This paper serves as the first paper of a sequel. In this sequel, we will investigate how thermodynamic laws are derived from billiards-like deterministic dynamics. The goal of this paper is to numerically justify that the deterministic dynamics of a billiards-like dynamical system is well-approximated by a Markovian energy exchange process. We carry out a series of numerical simulations to determine the rule of stochastic energy exchanges. Then we will use computer-assisted method proposed in [20] to justify that the resultant stochastic energy exchange model preserves many key properties of the original deterministic dynamics, such as ergodicity and thermal conductivity.

Consider many gas particles in a long and thin tube as in Figure 1 (top). Assume further that two ends of the tube is connected to heat baths with different temperatures. For the sake of simplicity, we assume gas particles only do free motion

and elastic collisions. When a particle hits the left (or right) boundary, a random particle drawn from a Boltzmann distribution is chosen to collide with this particle. Besides that, everything else is purely deterministic. Needless to say, any analysis of such a multi-body problem is extremely difficult. However, usually a gas particle collide with other particles very frequently. At ambient pressure, the mean free path of a gas molecule is as short as 68 nm. Therefore, motivated by earlier studies [2, 12, 11, 13], we propose to simplify the model by localizing gas molecules in a chain of cells as in Figure 1 (bottom). Disk-shaped particles are assumed to be trapped in those 2D cells, each of which is a chaotic billiard table with dispersive boundary. Adjacent cells are connected by a “gate”. Particles can not pass the “gate” but can collide through it. This gives the *nonequilibrium billiard model* introduced in Section 2. Throughout this paper, we assume that each cell contains M particles. M is a fixed finite number.

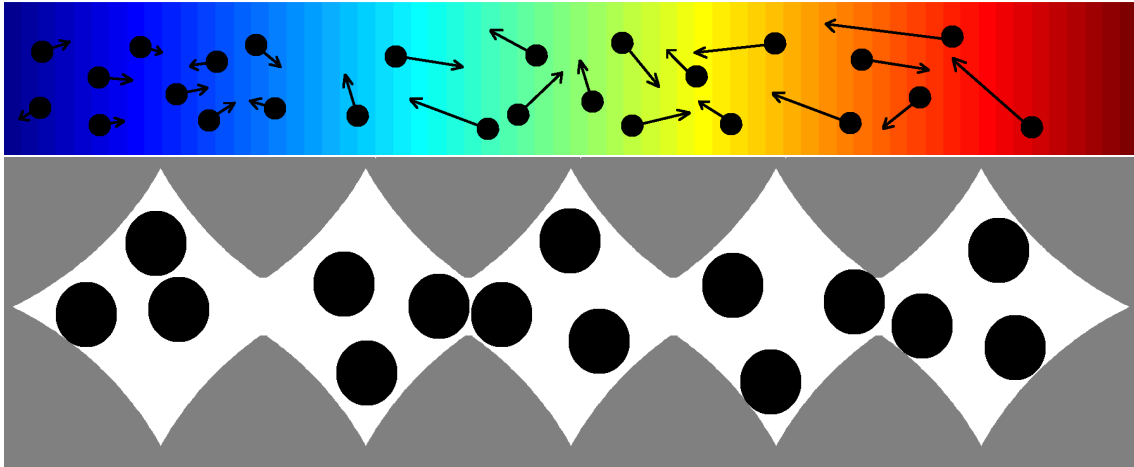


FIGURE 1. Top: Gas molecules in a tube. Bottom: Particles are trapped in a chain of cells. Particles can collide through the “gate”.

Since the motion of gas particles is highly chaotic, a particle has quick loss of memory. In fact, it is known that a chaotic billiard system usually have good statistical properties [4, 5, 6, 7]. This is a heuristic argument why we believe a Markov model should well approximate such a billiard model. In order to make the billiard model mathematics tractable, instead of modeling each particle, we choose to seek for a Markov process that describes the time evolution of total energy stored in each cell. When particles in neighbor cells collide, we let the corresponding cells exchange a certain random amount of energy. We call it a *stochastic energy exchange model*. Due to the significant difficulty of studying a multibody billiard system, a rigorous derivation of this Markov process is not possible. Instead, we use numerical simulation to justify this model reduction.

One needs to answer two questions in order to find the rule of stochastic energy exchange model: *when* and *how* two particles in neighbor cells exchange energy. To answer these questions, a series of numerical studies are carried out in Section 3. We find that the time of next collision between particles from adjacent cells is

not visually distinguishable from an exponential random variable. Therefore, one exponential clock should be associated with each adjacent pair of cells. The rate of this exponential clock is approximately square root of the minimum of two energies at the tail, as low total energy in a cell is always associated with long duration between two energy exchanges. The rule of energy exchange is more complicated. After some numerical simulations, we find a simple rule that can preserve qualitative properties that we are interested in. The energy of the particle that participates the collision satisfies the Beta distribution. After the collision, the energy is uniformly redistributed. Although this is not exactly the same case of the billiard system, it is simple enough while preserves the tail distribution on the low energy side, which determines the asymptotic properties of the system.

The stochastic energy exchange model is then summarized in the end of Section 3. Then we compared those two models from the aspects of ergodicity and thermal conductivity. In Section 4, we numerically showed that both models has polynomial ergodicity $\sim t^{-2M}$, where M is the number of particles in each cell. Note that a direct simulation of decay of correlation is not possible. For the billiard model, we use Monte Carlo simulation to compute the first passage time to a “high-energy state”, same as done in [18]. For the stochastic energy exchange model, we adopt the hybrid method proposed in [20], which replaces some key estimations in the rigorous proof of ergodicity of a Markov process by numerical simulations. Finally, in Section 5, we computed the thermal conductivity of the stochastic energy exchange model. We find that the thermal conductivity is proportional to $1/N$, which is consistent with early study of the billiard model in [12, 11] (with one particle in each cell).

2. NONEQUILIBRIUM BILLIARD MODEL FOR MICROSCOPIC HEAT CONDUCTION

As discussed in the introduction, it is difficult to study the dynamics when a large number of gas molecules moves and interacts in a tube. Since the mean free path of a gas molecule is very short, we “localize” gas molecules into a chain of cells. The precise description of this locally confined particle system is as follows.

Consider an 1D chain of N connected billiard tables in \mathbb{R}^2 , denoted by $\Omega_1, \dots, \Omega_N$. Each table is a subset of \mathbb{R}^2 whose boundary is formed by finitely many piecewise C^3 curves. Neighbor billiard tables are connected by one or finitely many “bottle-neck” openings. The first and the last tables are connected to the heat bath. The interaction with the heat bath will be described later.

Let M be a positive integer that is fixed throughout this section. Assume inside each billiard table there are M rigid moving disks with mass 2 and radius R . Each particle moves freely until it hits the boundary of the billiard table, or other particles. The configuration of a state of particles in the n -th cell is denoted by $(\mathbf{x}_1^n, \mathbf{v}_1^n, \dots, \mathbf{x}_M^n, \mathbf{v}_M^n)$, where $\mathbf{x}_k^n \in \mathbb{R}^2$ and $\mathbf{v}_k^n \in \mathbb{R}^2$ are the position (of the center) and velocity of the k -th particle in the n -th cell respectively. We assume the following for this billiard system.

- A particle is trapped in the cell in a way that its trajectory will never leave Ω_n .

- Particles in neighbor cells can collide with each other without passing through the opening between cells.
- All collisions are rigid body collisions. Particles do not rotate.
- Let $\Gamma_n \subset \Omega_n$ be the collection of possible positions of particles in the n -th table. There exist positions $\mathbf{x}_1^n, \dots, \mathbf{x}_M^n$ and $\epsilon > 0$ such that

$$|\mathbf{x}_i^n - \mathbf{x}_j^n| > 2R + \epsilon \text{ for all } i, j = 1 \sim M, i \neq j$$

and

$$\bigcup_{i=1}^M B(\mathbf{x}_i^n, R + \epsilon) \subset \Gamma_n \setminus \bigcup_{|m-n|=1} B(\Gamma_m, R).$$

In other words particles in a table can be completely out of reach by their neighbors. In addition a cell is sufficiently large such that particles won't get stuck.

Now we couple this chain with two heat baths. The temperature of two heat baths are T_L and T_R respectively. We assume that the heat bath is a billiard table with the same geometry and the same number of moving particles. But the total energy in the heat bath is randomly chosen. The rule of the heat bath interaction is the following. In the beginning a random total energy E_L (resp. E_R) is chosen for the left (resp. right) heat bath from the exponential distribution with mean T_L (resp. T_R). The initial distribution of particle positions and velocities satisfies the conditional Liouville measure (conditioning with the total energy E_L). This system is evolved deterministically until the first collision between a heat bath particle and a “regular” particle in the leftmost (resp. rightmost) table. Immediately after such a collision, particles in the heat bath are independently redistributed with a new total energy and new initial positions/velocities, which are drawn from the same distribution. This is an idealized way to approximate the interaction with a heat bath that has infinitely many particles.

Let

$$\Omega = \{(\mathbf{x}_1^1, \mathbf{v}_1^1, \dots, \mathbf{x}_M^1, \mathbf{v}_M^1), \dots, (\mathbf{x}_1^N, \mathbf{v}_1^N, \dots, \mathbf{x}_M^N, \mathbf{v}_M^N)\} \subset \mathbb{R}^{4MN}$$

be the state space of this billiard model. Let $\Phi_t : \Omega \rightarrow \Omega$ be the flow generated by the billiard model. It is easy to see that Φ_t is a piecewise deterministic Markov process.

3. REDUCTION TO STOCHASTIC ENERGY EXCHANGE MODEL

In order to make the nonequilibrium billiard model introduced in Section 2 tractable for further rigorous studies, we need to consider the evolution of some coarse-grained variables instead of velocities and positions of all particles. As introduced in the introduction, we seek for a Markov process that describes the time evolution of total energy stored in each cell. The aim of this section is to provide numerical justifications of such reduction from the deterministic billiard model to a stochastic energy exchange model. In the following two subsections, we study *when* and *how* an energy exchange between two adjacent cells, i.e., a collision between two particles from each cell respectively, should happen. The setting of our numerical simulation is as

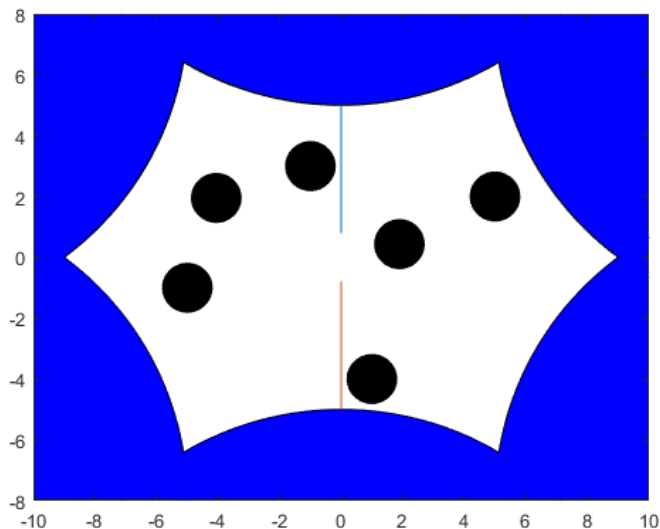


FIGURE 2. Setting of our numerical simulations. Two adjacent cells with three particles in each cell. Particles can collide through the gate, but can't pass through the gate.

follows. The boundary of two cells are determined by 6 circles and 2 line segments as seen in Figure 2. In each cell, there are $M = 2, 3, 4 \dots$ particles undergoing free motion and elastic collisions. We use Monte Carlo simulation to study the distribution of collision times and the distribution of energy transfer during a collision.

3.1. Distribution of collision time. The first numerical result is about the time distribution of energy exchanges between particles from neighboring cells, called the *collision time*. Heuristically, the deterministic billiard model is highly chaotic, which indicates a quick decay of correlation. This is the main motivation for us to look for its Markovian approximation. Due to the quick correlation decay, collision times between particles from adjacent cells should be close to a inhomogeneous Poisson process. This is to say, when starting from a fixed energy configuration, the first collision time should be well-approximated by an exponential distribution. Further, conditioning on the same energy configuration, time duration between two consecutive collisions should also satisfy an exponential distribution with the same rate. In dynamical systems, these two distributions are called the *hitting time* and the *return time*. It is known that for a strongly mixing dynamical system, those two times to an asymptotically small set coincides [15, 16]. We provide the following simulations to study distributions of the hitting time and the return time of the billiard model.

Rate of hitting time. Define the random variable

$$\tau_c = \inf\{t > 0 \mid \text{a cell-cell collision occurs at time } t\}.$$

If the collision time is Poisson, we should have

$$P(\tau_c > t) = \int_t^{+\infty} \lambda e^{-\lambda x} dx = e^{-\lambda t}.$$

In other words the rate of this Poisson distribution is $\lambda = -\frac{1}{t} \log P(\tau_c > t)$. However, the collision time is not Poisson because the energy process produced by the billiard model is clearly not Markovian. Instead, we use simulations to show that τ_c has an exponential tail, and define the slope of such tail by the stochastic energy exchange rate. More precisely, we study

$$\lim_{t \rightarrow \infty} -\frac{1}{t} \log P(\tau_c > t).$$

Consider an energy configuration (E_1, E_2) that correspond to total cell energy E_1 and E_2 in the left cell and right cell respectively. Further we assume that the initial distribution of particle positions and velocities satisfies the conditional Liouville measure. A function $R(E_1, E_2)$ is called the *stochastic energy exchange rate* if

$$\begin{aligned} R(E_1, E_2) &= \lim_{t \rightarrow \infty} -\frac{1}{t} \log P_\pi[\tau_c > t | \sum_{i=1}^M |\mathbf{v}_i^1|^2 = E_1, \sum_{j=1}^M |\mathbf{v}_j^2|^2 = E_2] \\ &= \lim_{t \rightarrow \infty} -\frac{1}{t} \log P_\pi[\tau_c > t | \sum_{i=1}^M |\mathbf{v}_i^1(0^+)|^2 = E_1, \sum_{i=1}^M |\mathbf{v}_i(0^+)|^2 = E_2, \\ &\quad \mathbf{x}_i^1 \in \text{int}(\Gamma_1), \mathbf{x}_j^2 \in \text{int}(\Gamma_2), |\mathbf{x}_i^1(0^+) - \mathbf{x}_j^2(0^+)| = 2r \text{ for some } 1 \leq i, j \leq M] \end{aligned}$$

is well-defined. The two limits in the definition give tails of the first collision time and the time between consecutive collisions, respectively.

Note that obviously $R(\alpha E_1, \alpha E_2) = \alpha^{1/2} R(E_1, E_2)$, we only need to simulate the case of $E_1 + E_2 = 1$. Without loss of generality we assume $E_1 \leq E_2$. We use Monte Carlo simulation to compute τ_c for the case of $M = 2, 3, 4$, with 28 energy configurations in each case. $R(E_1, E_2)$ versus E_1 for all three cases are plotted in Figure 3. We are interested in the scaling of R as $E_1 \rightarrow 0$. From the slope in the log-log plot in Figure 3, we can see that $R(E_1, E_2) \sim \sqrt{\min\{E_1, E_2\}}$ when $\min\{E_1, E_2\} \ll 1$ in all three cases.

Hitting time vs. return time. It remains to verify that the second limit in the definition of $R(E_1, E_2)$ gives the same tail. This is to say, we need to check that when conditioning on the same energy configuration, the distribution of time duration between two consecutive collision times, called the *conditional return time*, has the same exponential tail. Let $(E_1^{(1)}, E_2^{(1)}, t^{(1)}), (E_1^{(2)}, E_2^{(2)}, t^{(1)} + t^{(2)}), \dots, (E_1^{(N)}, E_2^{(N)}, t^{(1)} + \dots + t^{(N)})$ be a long trajectory sampled at collision times from a simulation starting from \mathbf{x}_0 . Same as in [18], we expect to have a joint probability density function $\rho_{\mathbf{x}_0}(E_1, E_2, t)$ about the conditional return time and the energy configuration. Further, if $R(E_1, E_2)$ is well-defined, we should have

$$\lim_{t \rightarrow \infty} \frac{1}{t} \log \left(\int_t^\infty \rho_{\mathbf{x}_0}(E_1, E_2, s) |_{(E_1, E_2)} ds \right) = R(E_1, E_2).$$

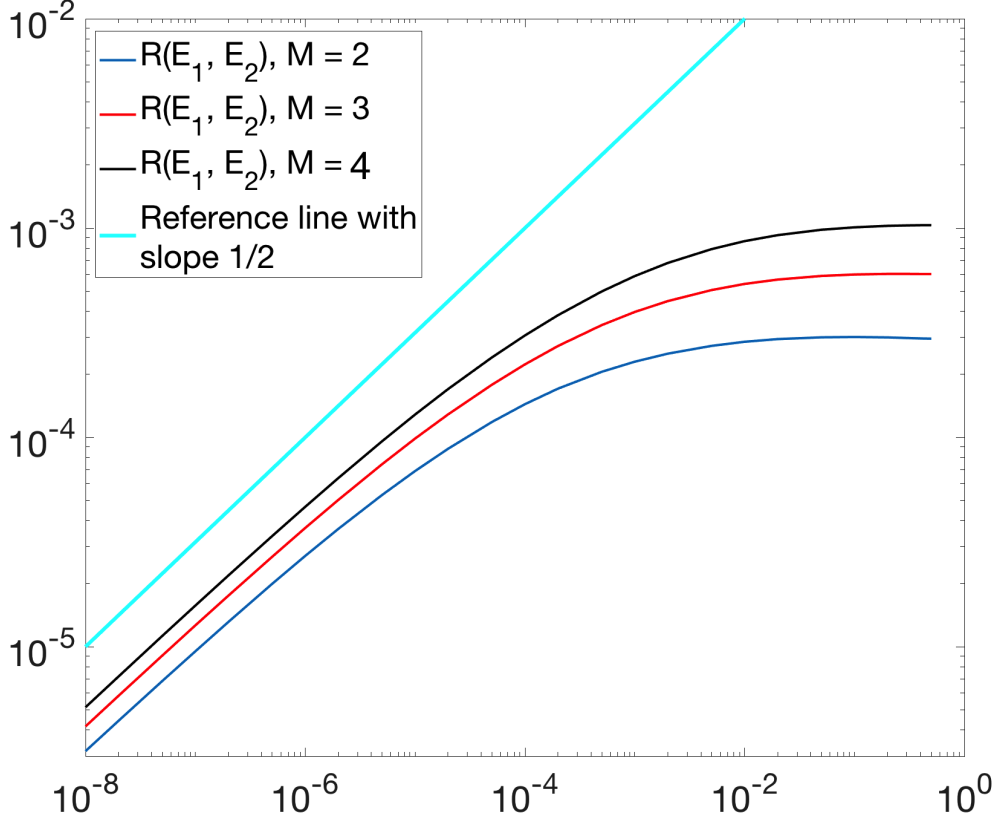


FIGURE 3. $R(E_1, E_2)$ versus E_1 in log-log plot for $M = 2, 3, 4$. $E_2 = 1 - E_1$.

We define the following rescaled return time

$$\Lambda(t) = \int_t^\infty \rho_{x_0}(E, 1 - E, s) R(E, 1 - E) dE ds.$$

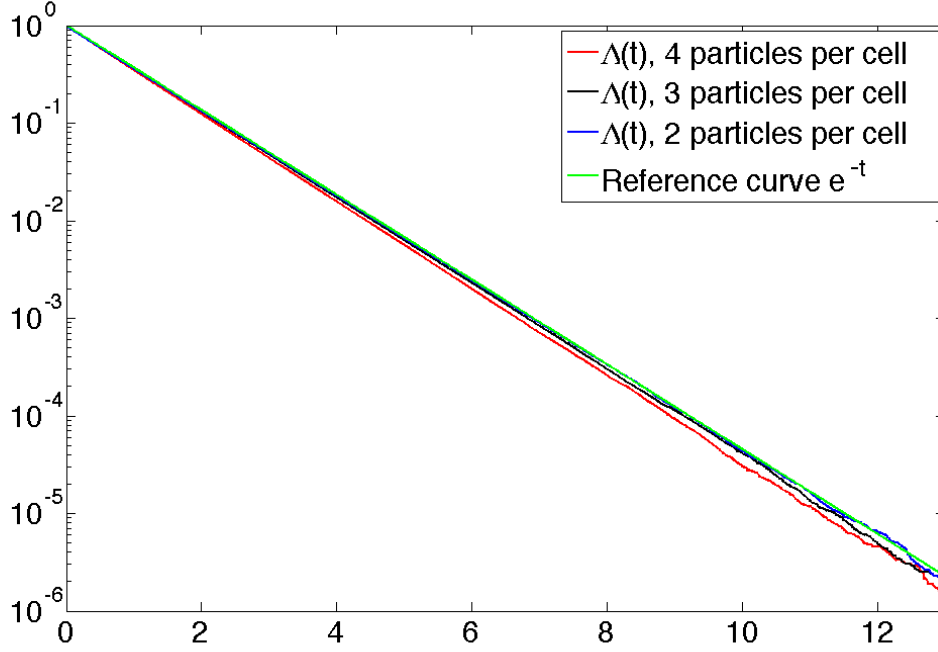
If the tail of $\rho_{x_0}(E_1, E_2, s)|_{(E_1, E_2)}$ has a slope $R(E_1, E_2)$, $\Lambda(t)$ should have a tail e^{-t} . It is easy to see that $\Lambda(t)$ can be sampled by $\{t^i R(E_1^{(i)}, E_2^{(2)})\}$, where $R(E_1, E_2)$ is obtained from Figure 4. We compare

$$\hat{\Lambda}(t) = \frac{1}{N} \left| \{t^i R(E_1^{(i)}, E_i^{(2)}) > t\} \right|$$

and e^{-t} in Figure 4 for $M = 2, 3, 4$. This verifies that the conditional return time coincides with the first collision time.

3.2. Rule of energy exchange. The second simulation is to study the rule of energy exchange at a collision. We separate this problem into two parts:

- (a) The energy distribution of a particle that participates in a collision.
- (b) The rule of the energy redistribution during the collision.

FIGURE 4. $\Lambda(t)$ from long trajectories for $M = 2, 3, 4$.

If there is only one particle in a cell, (a) becomes trivial. Otherwise, consider M particles collide with each other in a dispersive billiard table. Then it is natural to assume that the velocity distribution of these M particles is a uniform distribution on $(2M-1)$ -sphere. After some calculation, it is easy to see that the energy distribution of a particle is a Beta distribution with parameters $(1, M-1)$.

Proposition 3.1. *Let (X_1, \dots, X_{2M}) be a uniform distribution on the surface \mathbb{S}^{2M-1} . Then $X_1^2 + X_2^2$ has Beta distribution with parameters $(1, M-1)$.*

Proof. Let Y_1, \dots, Y_{2M} be $2M$ standard normal random variables. Let

$$X_i = \frac{Y_i}{\sqrt{Y_1^2 + \dots + Y_{2M}^2}}.$$

Then it is well known that (X_1, \dots, X_{2M}) gives a uniform distribution on the surface of a unit $(2M-1)$ -sphere. Therefore, we have

$$X_1^2 + X_2^2 = \frac{Y_1^2 + Y_2^2}{\sum_{i=1}^{2M} Y_i^2} := \frac{\Gamma_1}{\Gamma_1 + \Gamma_2},$$

where Γ_1 is a $\Gamma(1, 2)$ distribution and Γ_2 is a $\Gamma(M-1, 2)$ distribution. The ratio $\Gamma_1/(\Gamma_1 + \Gamma_2)$ is a Beta distribution with parameters $(1, M-1)$. \square

However, the energy distribution of the particle that participates in the collision is not a Beta distribution. It is obvious that faster particles have higher chance to

participate in such a collision. Hence the distribution should be biased towards high energy states.

Since the billiard system in each cell is assumed to be sufficiently chaotic, it is reasonable to assume that particles in neighboring cells are independent. Consider a pair of consecutive billiard tables. Let E_1 and E_2 be the total kinetic energy stored in the left and right local systems respectively. Let x_L and x_R be the ratio of the energy of the colliding particle to the total local energy. Because of the independence assumption, the probability density of x_L should be proportional to $A(t)$, where t is the “effective time” that a particle from the right table is available for a collision, and $A(t)$ is the area swiped by a particle during the time $(0, t)$.

It is obvious that

$$A(t) = \pi R^2 + 2R|v|t,$$

where $|v| = \sqrt{E_1 x_L}$. It is not easy to give an explicit expression of the “effective time”, but heuristically t should be proportional to

$$\frac{R}{\sqrt{E_2}} \cdot \frac{\sqrt{E_1}}{\sqrt{E_2}},$$

where the first term is the time duration that a particle from the right stays at the gate area, and the second term is the ratio of “time scales” in two cells. Hence we have

$$A(t) = \pi R^2 + 2CR^2 \frac{E_1}{E_2} \sqrt{x_L},$$

where C is a constant that depends on the geometry of the model. Combine with Proposition 3.1, we have approximation about the probability density of x_L .

$$(3.1) \quad p(x_L) = \frac{1}{K} (1 + C \frac{E_1}{E_2} \sqrt{x_L}) (1 - x_L)^{M-2}$$

if $M \geq 2$, where K is a normalizer.

This is verified by our numerical results. In Figure 5, we compare the approximation (3.1) with simulation results of x_L for three energy configurations $(E_1, E_2) = (0.1, 0.9)$, $(0.5, 0.5)$, and $(0.9, 0.1)$. The number of particles on each side is 4. The constant C is chosen to be 2.5. We can see that the approximation is quite close to the simulation result, especially when x_L is close to 1. Note that we are more interested in the distribution of x_L when it is close to 1 as it is related to the asymptotic dynamics of the full model.

Therefore, the energy of particles that participate in collision should be $E_1 B_1$ and $E_2 B_2$, where B_1 has the probability density function

$$\frac{1}{K} (1 + C \frac{E_i}{E_{i+1}} \sqrt{x}) (1 - x)^{M-2},$$

and B_2 has the probability density function

$$\frac{1}{K'} (1 + C \frac{E_{i+1}}{E_i} \sqrt{x}) (1 - x)^{M-2}.$$

To simplify the model, we only intend to capture the tail behavior of random variables B_1 , B_2 , and p . In other words, we would like to simplify the rule of energy

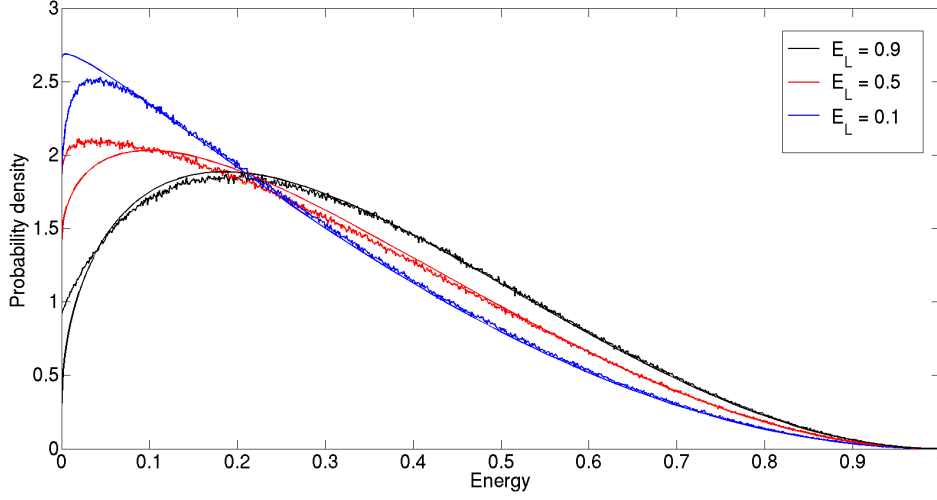


FIGURE 5. Energy distribution of particles participating in a collision.

exchange while preserving the right scaling when B_1 (or B_2) is close to 1. Since the correction term in $B_i, i = 1, 2$ does not affect the tail, we assume B_1 and B_2 are independent Beta distribution with parameters $(1, M - 1)$. This assumption is adopted throughout the rest of this paper.

The answer to (b) eventually boils down to the following questions. Consider two rigid disks moving and colliding in a “sufficiently chaotic” billiard table. If the initial kinetic energies are E_1 and E_2 but the initial position and direct of motion are both random, what will be the energy distribution of each particle after the first collision? Without loss of generality, we assume the velocities of two particles are

$$\mathbf{v}_1 = \sqrt{E_1}(\cos \alpha, \sin \alpha) \quad , \quad \mathbf{v}_2 = \sqrt{E_2}(\cos \beta, \sin \beta) \quad ,$$

respectively. Let the center of mass of two particles at their first collision be \mathbf{x}_1 and \mathbf{x}_2 . Similarly we let

$$\mathbf{x}_1 - \mathbf{x}_2 = 2R(\cos \gamma, \sin \gamma) \quad .$$

Assume two disks have equal mass and their mass center is the geometry center. Then it is well known that the post-collision velocities \mathbf{v}'_1 and \mathbf{v}'_2 are

$$\mathbf{v}'_1 = \mathbf{v}_1 - \frac{(\mathbf{v}_1 - \mathbf{v}_2, \mathbf{x}_1 - \mathbf{x}_2)}{\|\mathbf{x}_1 - \mathbf{x}_2\|^2}(\mathbf{x}_1 - \mathbf{x}_2)$$

and

$$\mathbf{v}'_2 = \mathbf{v}_2 - \frac{(\mathbf{v}_2 - \mathbf{v}_1, \mathbf{x}_2 - \mathbf{x}_1)}{\|\mathbf{x}_2 - \mathbf{x}_1\|^2}(\mathbf{x}_2 - \mathbf{x}_1) \quad ,$$

respectively. Since the total energy is conservative, it is sufficient to calculate $\|\mathbf{v}'_1\|^2$. Some calculation shows that

$$\|\mathbf{v}'_1\|^2 = E_1 \sin^2(\alpha - \gamma) + E_2 \cos^2(\beta - \gamma) \quad .$$

Therefore, we only need to find the joint distribution of $\alpha - \gamma$ and $\beta - \gamma$.

Let $\theta_1 = \alpha - \gamma$ and $\theta_2 = \beta - \gamma$. It is natural to assume that θ_1 and θ_2 are independently distributed on \mathbb{S}^1 . All we need to do is to find the conditional density of (θ_1, θ_2) when a collision happens. Without loss of generality, we rotate the coordinate such that $\mathbf{x}_1 - \mathbf{x}_2$ is horizontal. Now assume two particles are right before the first collision. It is easy to see that the time to collision is proportional to $(\sqrt{E_1} \cos \theta_1 - \sqrt{E_2} \cos \theta_2)^{-1}$ if $\sqrt{E_1} \cos \theta_1 - \sqrt{E_2} \cos \theta_2 > 0$, and ∞ otherwise. In other words, conditioning on having a collision, the density of (θ_1, θ_2) should be proportional to

$$(\sqrt{E_1} \cos \theta_1 - \sqrt{E_2} \cos \theta_2) \mathbf{1}_{\sqrt{E_1} \cos \theta_1 - \sqrt{E_2} \cos \theta_2 > 0}.$$

Therefore, the post-collision kinetic energy of particle 1 equals

$$E_1 \sin^2(\theta_1) + E_2 \cos^2(\theta_2),$$

where (θ_1, θ_2) has a joint probability density function

$$\frac{1}{L} (\sqrt{E_1} \cos \theta_1 - \sqrt{E_2} \cos \theta_2) \mathbf{1}_{\sqrt{E_1} \cos \theta_1 - \sqrt{E_2} \cos \theta_2 > 0},$$

where L is a normalizer.

This is justified by the numerical simulation result. In Figure 3.2, we demonstrated the energy distribution of the left particle after a collision with starting from random initial position, random initial direction, and fixed left/right particle energies. This matches exactly our analysis about the post-collision energy distribution.

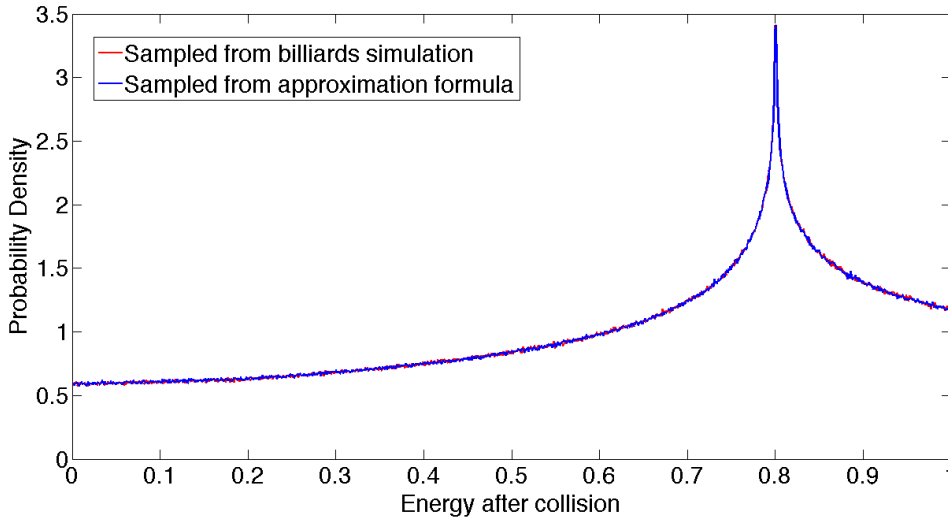


FIGURE 6. Energy distribution after a collision. Per-collision energy: left particle 0.2, right particle 0.8.

It is difficult to give an explicit expression of the distribution of $\|\mathbf{v}_1\|^2$. However, it is not hard to show that for each strictly positive energy pair (E_1, E_2) , $\|\mathbf{v}_1\|^2$ has strictly positive density everywhere. Same as in (a), we look for a simple expression that preserves the tail dynamics, which is essentially the tail probability that E_1 (or

E_2) is very small after an energy exchange. Therefore, for the sake of simplicity, we assume that the energy redistribution is given in a “random halves” fashion, i.e.,

$$(E'_1, E'_2) = (p(E_1 + E_2), (1 - p)(E_1 + E_2)),$$

where p is uniformly distributed on $(0, 1)$. This assumption is valid throughout the rest of this paper.

Our numerical simulation shows that this simplification preserves the same tail distribution as well as the same scaling of the energy current. In Figure 7, we show the probability density function of post-collision left cell energy when 3 particles on each side starting with an energy configuration $(E_1, E_2) = (0.5, 0.5)$. One can see a quadratic tail of the density function. This means $\mathbb{P}[E'_1 < \epsilon] \sim \epsilon^3$. Finally, in Figure 8 we showed the average energy flux when each side has 3 particles and the total energy is set to be 1. We can see that the energy flux is proportional to the difference of cell energy, which further supports the simplified rule of energy exchange.

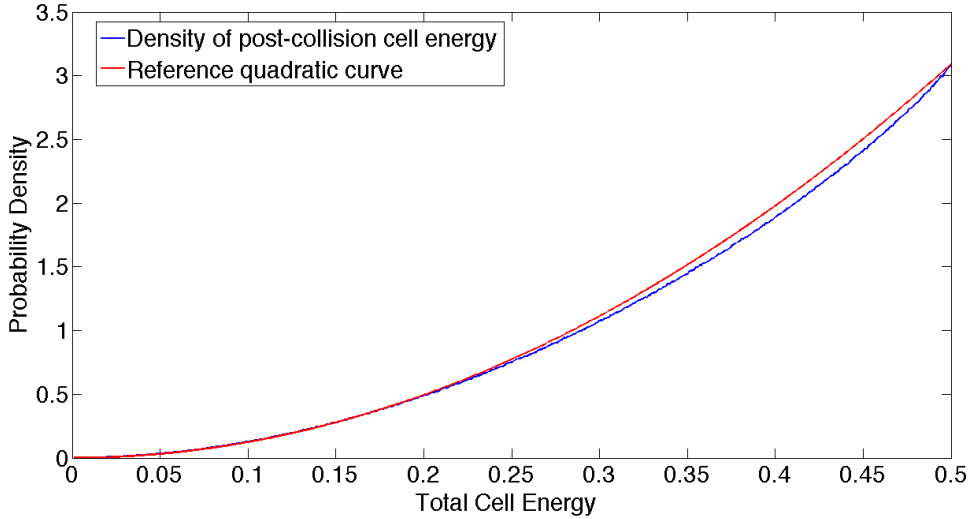


FIGURE 7. Probability density function of total cell energy after a collision. Number of particles on each side = 3.

In summary, let E_i and E_{i+1} be the total local energy in two neighboring tables, the rule of energy exchange is the following.

$$(E'_i, E'_{i+1}) = (E_i - (1 - p)E_i B_1 + pE_{i+1} B_2, E_{i+1} - pE_{i+1} B_2 + (1 - p)E_i B_1),$$

where B_1 and B_2 are two Beta distribution with parameters $(1, M - 1)$, and p has uniform positive density on $(0, 1)$. Moreover, B_1 , B_2 , and p are independent.

3.3. Stochastic energy exchange model. In summary, the qualitative properties of the nonequilibrium billiard model is preserved by the following *stochastic energy exchange model*.

Consider a chain with N sites that is connected to two heat baths. Let M be an integer that is the model parameter. Each site carries a certain amount of energy. Temperatures of two heat baths are assumed to be T_L and T_R respectively.

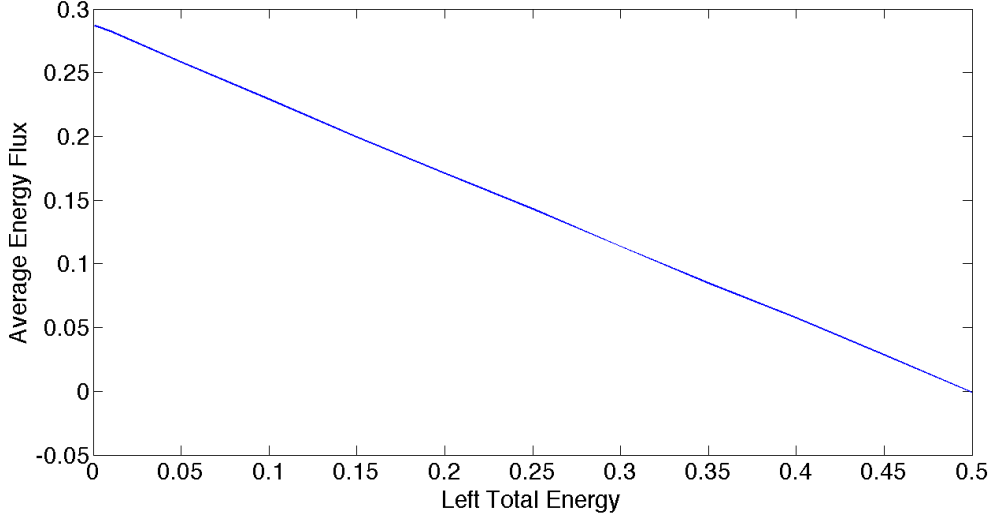


FIGURE 8. Average energy flux from right to left with changing energy configuration. Number of particles on each side = 3. x -axis is the total energy in the left cell. The total energy in the right cell is 1 minus the total energy in the left cell.

As discussed in Section 3.1, the energy exchange times can be approximated by a Poisson distribution. Hence an exponential clock is associated to a pair of sites E_i and E_{i+1} . The rate of the clock is $R(E_i, E_{i+1}) = \sqrt{\min\{E_i, E_{i+1}\}}$. When the clock rings, a random proportion of energy is chosen from each site. Then these energies are pooled together and redistributed back randomly. The random proportion satisfies a Beta distribution. More precisely, the rule of update immediately after a clock ring is

$(E'_i, E'_{i+1}) = (E_i - E_i B_1 + p(E_i B_1 + E_{i+1} B_2), E_{i+1} - E_{i+1} B_2 + (1-p)(E_i B_1 + E_{i+1} B_2))$, where B_1 and B_2 are two independent Beta random variables with parameters $(1, M-1)$, p is a uniform random variable on $(0, 1)$ that is independent with everything else.

We also need to describe the rule of interaction with the heat bath. Two more exponential clocks are associated to the left and the right heat baths. The rate of the left (resp. right) clock is $R(T_L, E_1)$ (resp. $R(E_N, T_R)$). When the clock ring, the rule of update is

$$\begin{aligned} E'_1 &= E_1 - E_1 B_1 + p(E_1 B_1 + X_L B_2), \\ (\text{resp.} \\ E'_N &= E_N - E_N B_1 + p(E_N B_1 + X_R B_2), \\) \end{aligned}$$

where X_L and X_R are exponential random variables with mean T_L and T_R respectively, p , B_1 , B_2 are same as before.

The stochastic energy exchange model generates a Markov jump process \mathbf{E}_t on \mathbb{R}_+^N . We denote P^t by the transition kernel of \mathbf{E}_t . We further define the left operator

of P^t acting on a probability measure μ

$$\mu P^t(A) = \int_{\mathbb{R}_+^N} \mu(dx) P^t(x, A)$$

and the right operator of P^t acting on a measurable function ξ

$$P^t \xi(x) = \int_{\mathbb{R}_+^N} P^t(x, dy) \xi(y).$$

4. ERGODICITY OF NONEQUILIBRIUM STEADY STATE

4.1. Ergodicity of the stochastic model. We claim that we have convincing numerical evidence to show that the stochastic model has a t^{-2M} speed of contraction and $t^{-(2M-1)}$ speed of convergence to its steady state. A rigorous proof of such polynomial ergodicity roughly follows the approach developed in [23], which is very tedious and technical. We choose to show it numerically in the present paper and write a separate paper for the proof of the polynomial ergodicity of the stochastic energy exchange model.

It is very difficult to show the speed of convergence through a direct Monte Carlo simulation. The decay of correlation has small expectation but $O(1)$ variance. To reduce the relative error, a huge amount of samples will be necessary. If the speed of convergence is slow, such a simulation becomes impractical. Instead, we adopt the hybrid approach proposed in [20].

Let Ψ_n^h be the time- h sample chain of a continuous time Markov process Ψ_t on a measurable space (X, \mathcal{B}) . Let $\mathcal{P}(x, \cdot)$ be the transition kernel of Ψ_n^h . Further define

$$\tau_A(h) = \inf_{t \geq h} \{\Psi_t \in A\}.$$

By [20], in order to show the polynomial ergodicity of Ψ_t , we need the following four analytical conditions and two numerical conditions.

(A1) Ψ_n^h is *irreducible* with respect to a non-trivial probability measure ϕ . In other words for any $x \in X$ and any $A \in \mathcal{B}$ with $\phi(A) > 0$, there exists an integer $n > 0$ such that $\mathcal{P}^n(x, A) > 0$.

(A2) Ψ_n^h admits a *uniform reference set* \mathfrak{C} such that

$$P^h(x, \cdot) \geq \eta \theta(\cdot) \quad \text{for all } x \in \mathfrak{C},$$

where $\theta(\cdot)$ is a probability measure. In addition Ψ_n^h is *strongly aperiodic*, i.e., $\theta(\mathfrak{C}) > 0$

(A3) For any probability measure μ ,

$$\|\mu P^\delta - \mu\|_{TV} \rightarrow 0 \text{ as } \delta \rightarrow 0.$$

(A4) There exists $\gamma > 0$ such that

$$\inf_{x \in \mathfrak{C}} \inf_{t \in [0, h]} P_x[\Psi_t = \Psi_0] > \gamma.$$

(N1) Distributions $\mathbb{P}_\mu[\tau_{\mathfrak{C}}(h) \geq t]$ and $\mathbb{P}_\pi[\tau_{\mathfrak{C}}(h) \geq t]$ have polynomial tails $\sim t^{-\beta}$ for some $\beta > 1$, where π is the numerical invariant measure of Φ_t .

(N2) Function

$$\gamma(x) = \sup_{t \geq h} \frac{\mathbb{P}_x[\tau_{\mathfrak{C}}(h) > t]}{t^{-\beta}}$$

is uniformly bounded on \mathfrak{C} .

In [20], we have showed that conditions (A1) – (A4), (N1), and (N2) implies the following conclusions.

- (a) Ψ_t admits an invariant probability measure π .
- (b) Polynomial convergence rate to π :

$$\lim_{t \rightarrow \infty} t^{\beta-\epsilon} \|\mu \mathcal{P}^t - \pi\|_{TV} = 0$$

for any $\epsilon > 0$.

- (c) Polynomial decay rate of correlation:

$$\lim_{t \rightarrow \infty} t^{\beta-\epsilon} C_{\mu}^{\xi, \eta} = 0$$

for any $\epsilon > 0$ and probability measure μ satisfying (N1), where

$$C_{\mu}^{\xi, \eta}(t) := \left| \int (\mathcal{P}^t \eta)(x) \xi(x) \mu(dx) - \int (\mathcal{P}^t \eta)(x) \mu(dx) \int \xi(x) \mu(dx) \right|.$$

- (d) Polynomial convergence rate to π . For any $\epsilon > 0$, we have

$$\lim_{t \rightarrow \infty} t^{\beta-\epsilon} \|\delta_x \mathcal{P}^t - \pi\|_{TV} = 0$$

for ϕ -almost every $x \in X$.

- (e) Polynomial speed of contraction. For any $\epsilon > 0$, we have

$$\lim_{t \rightarrow \infty} t^{\beta-\epsilon} \|\delta_x \mathcal{P}^t - \delta_y P^t\|_{TV} = 0$$

for ϕ -almost every $x, y \in X$.

Note that we did not specify conclusion (e) in [20]. But (e) is a natural corollary of Proposition 4.1 of [20], which implies $\mathbf{E}_x[\tau_{\mathfrak{C}}^{\beta}] < \infty$ for ϕ -almost $x \in X$.

4.2. Verifying analytical conditions. We will first work on the time- h chain \mathbf{E}_n . The verification of condition (A1) for \mathbf{E}_n is based on the following Theorem.

Theorem 4.1. *For any set $K \subset \mathbb{R}_+^N$ of the form $K = \{(e_1, \dots, e_N) \mid 0 < c_i \leq e_i \leq C_i, i = 1 \sim N\}$ and any $h > 0$, there exists a constant $\eta > 0$ such that*

$$P(\mathbf{E}, \cdot) > \eta U_K(\cdot),$$

for any $\mathbf{E} \in K$, where U_K is the uniform probability distribution over K .

Proof. This proof is similar to Theorem 5.1 of [20]. We include the proof here for the completeness of the paper. Consider any two points $\mathbf{E}^* = \{e_1^*, \dots, e_N^*\} \in K$ and $d\mathbf{E} = \{(de_1, \dots, de_N), de_i > 0, i = 1 \sim N\}$. Assume $0 < de_i \ll 1$. Let

$$B(\mathbf{E}^*, d\mathbf{E}) = \{(x_1, \dots, x_N) \in \mathbb{R}^N \mid e_i^* \leq x_i \leq e_i^* + de_i^*\}$$

be a small hypercube close to \mathbf{E}^* . It then suffices to prove that for any $\mathbf{E}_0 = \{\bar{e}_1, \dots, \bar{e}_N\} \in K$, we have

$$(4.1) \quad P(\mathbf{E}_0, B(\mathbf{E}^*, d\mathbf{E})) > \sigma de_1 de_2 \cdots de_N,$$

where σ is a strictly positive constant that only depends on K .

We will then construct the following sequence of events to go from the state \mathbf{E}_0 to $B(\mathbf{E}^*, d\mathbf{E})$ with desired positive probability. Denote the process starting from \mathbf{E}_0 by $\mathbf{E}_t = (e_1(t), \dots, e_N(t))$. Let $\delta = \frac{h}{2N+1}$ and let $\epsilon > 0$ be sufficiently small such that $\epsilon < \min\{c_i, i = 1 \sim N\}$. Let $H = \sum_{i=1}^N (e_i^* + de_i)$. We consider events $A_1 \dots, A_N$ and B_1, \dots, B_{N+1} , where A_i and B_j specifies what happens on the time interval $(i\delta, (i+1)\delta]$ and $(N\delta + (j-1)\delta, N\delta + j\delta]$, respectively.

- $A_i = \{e_i(i\delta) \in [\epsilon/2, \epsilon]\}$ and $\{ \text{the } i\text{-th clock rings exactly once, all other clocks are silent on } ((i-1)\delta, i\delta] \}$.
- $B_1 = \text{Energy emitted by right heat bath} \in (H, 2H)$ and the N -th clock rings exactly once, all other clocks are silent on $(N\delta, (N+1)\delta]$.
- $B_j = \{e_j(N\delta + j\delta) \in [e_{N+2-j}^*, e_{N+2-j}^* + de_j]\}$ and $\{ \text{the } (N+1-j)\text{-th clock rings exactly once, all other clocks are silent on } (N\delta + (j-1)\delta, N\delta + j\delta] \}$ for $j = 2, \dots, N+1$.

The idea is that the energy at each site is first transported to the right heat bath, with only an amount of energy between $\epsilon/2$ and ϵ left at each site (events $A_1 \sim A_N$). Then a sufficiently large amount of energy is injected into the chain from the right heat bath (event B_1) so that it is always possible for site j to acquire an amount of energy between e_j^* and $e_j^* + de_j$ by passing the rest to site $j-1$ (events $B_2 \sim B_{N+1}$), where sites 0 and $N+1$ denote the left and right heat baths respectively.

It is easy to show that for each parameter M , the probability of occurrence of the sequence of events described above is always strictly positive. Below is a sketch of calculation. We will leave detailed calculations to the reader.

- (a) After each energy exchange, the rate of clocks have a uniform lower bound $\epsilon/2$.
- (b) By the rule of energy redistribution, it is easy to see that the probabilities of A_i are strictly positive.
- (c) There is also a uniform upper bound on H given by $2 \sum_{i=1}^N C_i$.
- (d) From the rule of energy redistribution, the probability that $e_j(N\delta + j\delta) \in (e_j^*, e_j^* + de_j)$ after an energy exchange in event B_{j+1} is greater than αde_j for some strictly positive constant α . Hence probabilities of B_j are greater than $\text{const} \cdot de_j$.

In addition, all these probabilities are uniformly bounded from below for all \mathbf{E}^* and \mathbf{E}_0 in K . Hence we have

$$\mathbb{P}[A_1 \dots A_N B_1 \dots B_{N+1}] \geq \sigma de_1 \dots de_N$$

for some constant $\sigma > 0$. □

As a corollary, we can prove that \mathbf{E}_n is both aperiodic and irreducible with respect to the Lebesgue measure.

Corollary 4.2. \mathbf{E}_n is a strongly aperiodic Markov chain.

Proof. By theorem 4.1, K is a uniform reference set. In addition $U_K(K) > 0$. The strong aperiodicity follows from its definition. □

Therefore \mathbf{E}_n is aperiodic.

Corollary 4.3. \mathbf{E}_n is λ -irreducible, where λ is the Lebesgue measure on \mathbb{R}_+^N .

Proof. Let $A \subset \mathbb{R}_+^N$ be a set with strictly positive Lebesgue measure. Then there exists a set K that has the form $\{(e_1, \dots, e_N) \mid 0 < c_i \leq e_i \leq C_i, i = 1 \sim N\}$ and $U_K(K \cap A) > 0$.

For any $\mathbf{E}_0 \in \mathbb{R}_+^N$ and the time step $h > 0$, we can choose a $K \subset \mathbb{R}_+^N$ of the form $K = \{(e_1, \dots, e_N) \mid 0 < c_i \leq e_i \leq C_i, i = 1 \sim N\}$ for some $c_i > 0$ and $C_i < \infty$, such that $\mathbf{E}_0 \in K$. Same construction as in Theorem 4.1 implies that $P^h(\mathbf{E}_0, \cdot) > \eta U_K(\cdot)$ for some $\eta > 0$. Therefore, $P^h(\mathbf{E}_0, A) > \eta U_K(A) > 0$. \square

Hence assumption **(A1)** and **(A2)** are satisfied.

We can also prove the absolute continuity of π with respect to the Lebesgue measure, which is denoted by λ .

Proposition 4.4. *If π is an invariant measure of \mathbf{E}_t , then π is absolutely continuous with respect to λ with a strictly positive density.*

Proof. This proof is identical to that of Lemma 6.3 of [22]. \square

Condition **(A3)**, or “continuity at zero” follows from the following Proposition.

Proposition 4.5. *For any probability measure μ on \mathbb{R}_+^N ,*

$$\lim_{\delta \rightarrow 0} \|\mu P^\delta - \mu\|_{TV} = 0.$$

Proof. This proof is identical to that of Lemma 5.6 of [21]. \square

Condition **(A4)** is trivial as all clock rates are uniformly bounded in any compact set \mathfrak{C} .

4.3. Verifying numerical conditions. Now we are ready to present our numerical results. We let $N = 3$ and $M = 2$ in our simulations to demonstrate the result. The uniform reference set \mathfrak{C} is chosen as

$$\mathfrak{C} = \{(e_1, \dots, e_N) \mid 0.1 \leq e_i \leq 100, i = 1 \sim N\}.$$

Throughout our numerical justification, we let $h = 0.1$. (Recall that for a time-continuous Markov process Ψ_t , the definition of $\tau_{\mathfrak{C}} = \tau_{\mathfrak{C}}(h)$ depends on h .) Our numerical simulation shows that the tail of $\mathbb{P}_{\mathbf{E}}[\tau_{\mathfrak{C}} > t]$ is $\sim t^{-4}$ for many initial condition \mathbf{E} that we have tested. This is consistent with the heuristic argument. The tail of $\mathbb{P}_{\pi}[\tau_{\mathfrak{C}} > t]$ is a very subtle issue as an explicit formulation of π is not possible. We conjecture that $\mathbb{P}_{\pi}[\tau_{\mathfrak{C}} > t] \sim t^{-3}$.

We have the following argument and numerical evidence to support this conjecture. Consider the simplest case when $N = 1$. Let $\pi(\{E_1 < \epsilon\})$ have the tail ϵ^p for all sufficiently small ϵ . Then the density function at $E_1 = \epsilon$ is $\sim \epsilon^{p-1}$. Since π is invariant, for an infinitesimal $h > 0$, we have

$$O(h)\epsilon^M \approx O(h) \int_0^\epsilon s^{p-1} \sqrt{s} ds,$$

where the left term is the probability that $E_1 < \epsilon$ after one energy exchange within $(0, h)$, and the right term is the probability that E_1 exchanges energy with $(0, h)$. This implies $p = M - 1/2$.

We need to be very careful about the initial distribution when computing the numerical invariant probability measure, as it takes a long time for the model to correct the tail at low energy. Our strategy is to generate a numerical invariant probability measure from a initial distribution with a correct tail. Let $\mu_0 \sim (\rho_1, \dots, \rho_N)$, where ρ_i is an exponential distribution with mean $(T_L + T_R)/2$. We manually correct the tail of μ_0 before putting it into the Monte Carlo simulation. This manual correction gives a new initial distribution $\mu_1 \sim (\rho_1, \dots, \rho_N)$, where

$$\begin{cases} \rho_i \sim \mathcal{E}((T_L + T_R)/2) & \text{if } \mathcal{E}((T_L + T_R)/2) > 0.01 \\ \rho_i \sim 0.01u^{(M-1/2)^{-1}} & \text{otherwise} \end{cases},$$

and $\mathcal{E}(\lambda)$ means an exponential random variable with mean λ . The tail of $\mu_0 P^{200}$ and $\mu_1 P^{200}$ are compared in Figure 10. The expectation of E_2 versus time is plotted in Figure. We find that although expectations of many observables we have tested are stabilized when $T = 200$ (Figure 9), the low energy tail of μ_0 has not been stabilized. This problem is solved by using μ_1 . We choose $\hat{\pi} = \mu_1 P^{100}$ to be our numerical invariant measure. Our simulation shows that $\mathbb{P}_{\hat{\pi}}[\tau_{\mathfrak{E}} > t] \sim t^{-3}$. (Figure 11).

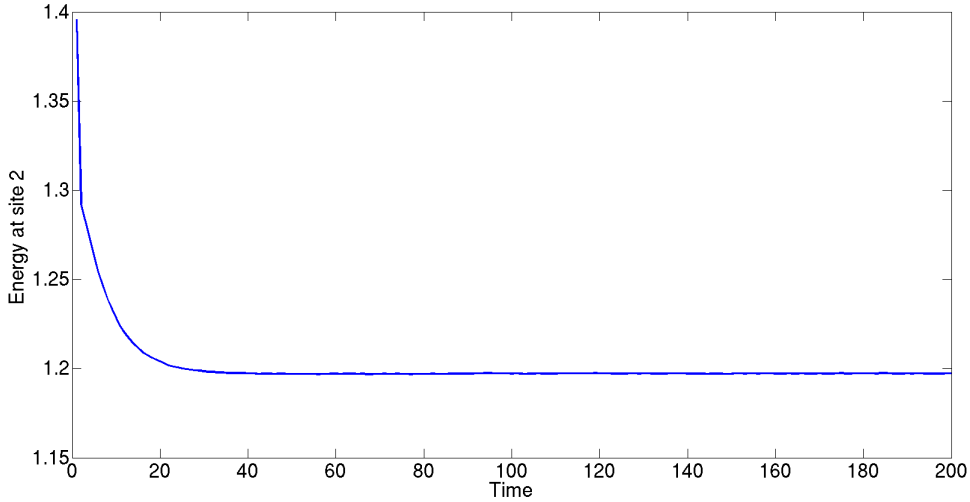


FIGURE 9. Expectation of E_2 vs. time with $N = 3$ and $M = 2$. Sample size of Monte Carlo simulation is 10^9 .

It remains to check **(N2)**. We numerically show that

$$\gamma(\mathbf{E}) = \sup_{t \geq h} \frac{\mathbb{P}_{\mathbf{E}}[\tau_{\mathfrak{E}} > t]}{t^{-4}}$$

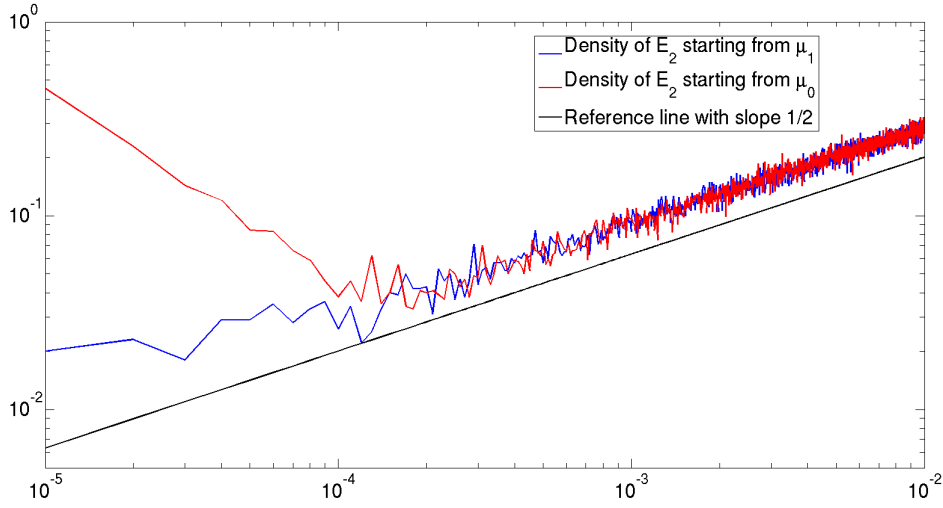


FIGURE 10. Density function of E_2 with starting from initial distribution μ_0 and μ_1 . We divide $[0, 0.01]$ into 1000 bins and count the number of E_2 falling into each bin. Sample size of Monte Carlo simulation is 10^9 .

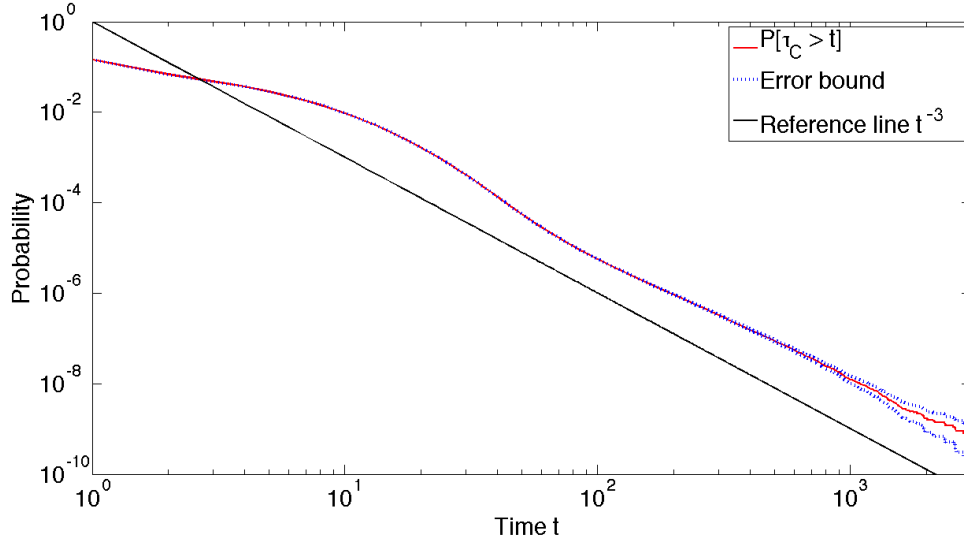


FIGURE 11. $\mathbb{P}[\tau_{\mathcal{C}} > t]$ versus t when starting from $\hat{\pi}$. Blue dots are the error bar with confidence level 0.95. Sample size of Monte Carlo simulation is 10^{10} .

is uniformly bounded on \mathfrak{C} . We follow procedure (a)-(d) in Section 4.1 to show the boundedness of $\gamma(\mathbf{E})$. In fact,

$$\gamma_N(\mathbf{E}) = \sup_{1 \leq n \leq N} \sup_{t \geq h} \frac{\mathbb{P}_{\mathbf{E}}[\tau_{\mathfrak{C}} > t]}{t^{-2}}$$

is stabilized very fast with increasing N . A sample of size 10^6 is sufficient for a reliable estimate of $\gamma(\mathbf{E})$. Figure 12 shows that when E_i is small, $\gamma(\mathbf{E})$ decreases monotonically with decreasing E_i for each $i = 1 \sim 3$. Therefore, we expect that the maximal of $\gamma(\mathbf{E})$ in \mathfrak{C} is reached at $\mathbf{E}_* = (0.1, 0.1, 0.1)$. In fact, intuitively one should expect $\gamma(\mathbf{E})$ to decrease with site energy as starting from low site energy means having higher probability to have even lower site energy after an energy exchange. Finally, we run the simulation again to estimate $\gamma(\mathbf{E}_*)$. As seen in Figure 13, when starting from \mathbf{E}_* the probability of return has tail $\sim t^{-4}$.

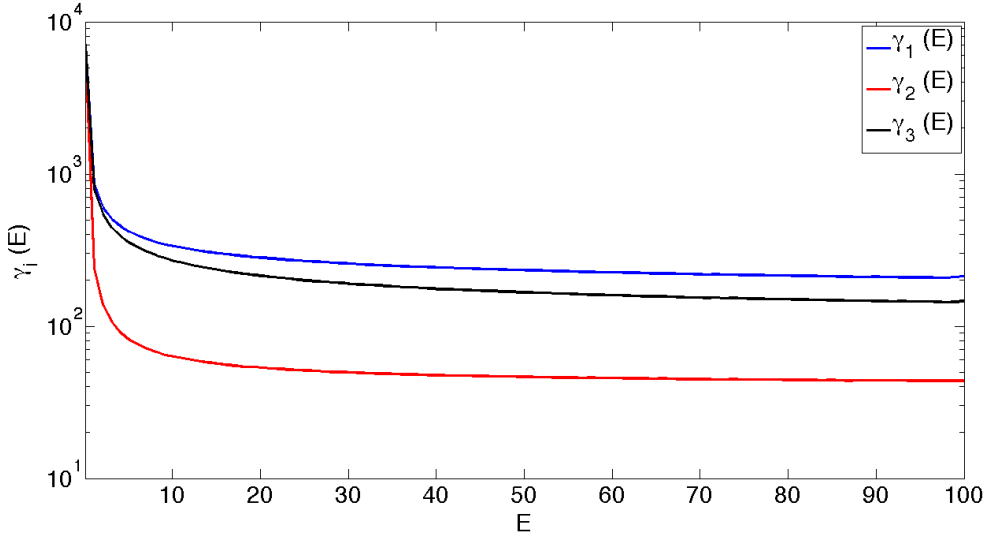


FIGURE 12. $\gamma_i(E)$ means replacing the i -th entry of $\gamma(0.1, 0.1, 0.1)$ by E . Three curves show the plot of $\gamma_i(E)$ on $[0.1, 100]$ for $i = 1 \sim 3$. We use linear-log plot because values of $\gamma_i(E)$ changes significantly when E is small.

4.4. Main conclusions. The previous subsection verifies two numerical conditions (N1) and (N2) for \mathbf{E}_t with parameter $2M$. The slopes of $\mathbb{P}_{\mathbf{E}^*}[\tau_{\mathfrak{C}} > t]$ and $\mathbb{P}_{\pi}[\tau_{\mathfrak{C}} > t]$ in the log-log plot are $2M$ and $2M - 1$ respectively.

We also need the uniqueness of π .

Proposition 4.6. *For any $h > 0$, \mathbf{E}_n^h admits at most one invariant probability measure.*

Proof. By the proof of Theorem 4.1, for any $\mathbf{E} \in K$, $P^{h/2}(\mathbf{E}, \cdot)$ has strictly positive density on K . In addition, $P^{h/2}(\mathbf{E}_0, K) > 0$ for any $\mathbf{E}_0 \in \mathbb{R}_+^N$. Hence $P^h(\mathbf{E}_0, \cdot)$ has positive density on K . This implies that every $\mathbf{E}_0 \in \mathbb{R}_+^N$ belongs to the same

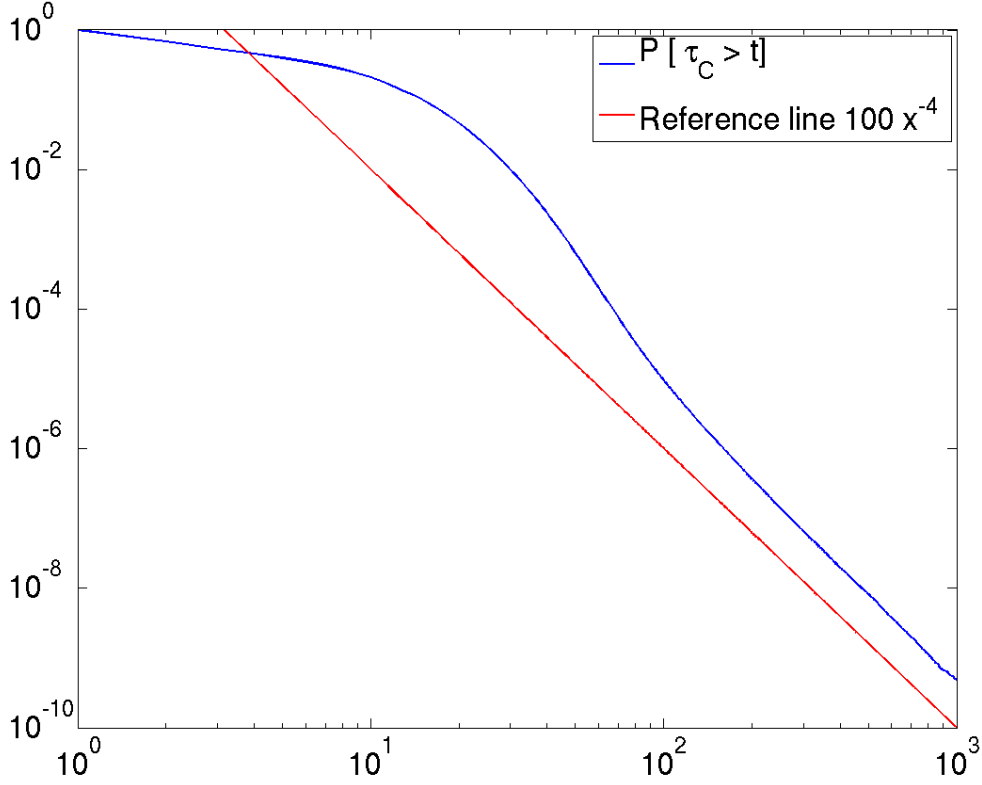


FIGURE 13. $\mathbb{P}[\tau_{\mathfrak{C}} > t]$ versus t when starting from E^* . Sample size of Monte Carlo simulation is 10^{10} .

ergodic component. Therefore \mathbf{E}_n^h cannot have more than one invariant probability measure. \square

In summary, we have the following conclusions for \mathbf{E}_t . Since now $P_x[\tau_{\mathfrak{C}} > t]$ and $P_\pi[\tau_{\mathfrak{C}} > t]$ have different tails, we can apply conclusions (a) - (e) with $\beta = 2M$ when π is not involved.

- (1) For any T_L, T_R , there exists a unique invariant probability measure π , i.e., the nonequilibrium steady-state, which is absolutely continuous with respect to the Lebesgue measure on \mathbb{R}_+^N .
- (2) For almost every $\mathbf{E}_0 \in \mathbb{R}_+^N$ and any sufficiently small $\epsilon > 0$, we have

$$\lim_{t \rightarrow \infty} t^{2M-1-\epsilon} \|\delta_{\mathbf{E}_0} P^t - \pi\|_{TV} = 0.$$

- (3) For any functions $\eta, \xi \in L^\infty(\mathbf{R}_+^N)$, we have

$$C_\mu^{\eta, \xi}(t) \leq O(1) \cdot t^{\epsilon-2M}$$

for any $\epsilon > 0$ and μ satisfies **(N1)**.

- (4) For almost every points $\mathbf{E}_0, \mathbf{E}_1 \in \mathbb{R}_+^N$ and any sufficiently small $\epsilon > 0$, we have

$$\lim_{t \rightarrow \infty} t^{2M-\epsilon} \|\delta_{\mathbf{E}_0} P^t - \delta_{\mathbf{E}_1} P^t\|_{TV} = 0.$$

4.5. Ergodicity of the billiard model. The ergodicity of the billiard model is very difficult to either prove or compute. Let Φ_t be the flow of the billiard model, μ be the initial measure, η and ξ be two observables. Theoretically the decay of correlation

$$C_{\xi, \eta}^\mu(t) = \int_X \xi(\Phi_t(x)) \eta(x) \mu(dx) - \int_X \xi(\Phi_t(x)) \mu(dx) \int_X \eta(x) \mu(dx)$$

is computable. The speed of decay of correlation gives the ergodicity of the billiard model. However, for large t $C_{\xi, \eta}^\mu(t)$ has very small expectation and $O(1)$ variance. In order to control the relative error, the sample size of Monte Carlo simulation needs to be very large. In particular, the polynomial tail usually can only be captured for large t . Simple calculation shows that the required sample size can easily exceed the ability of today's computer.

Instead, we choose to present other evidence to support the polynomial speed of correlation decay. The assumption is that when the total kinetic energy in both cells are sufficiently high, the decay of correlation is exponentially fast. Therefore, if the first passage time to such a high energy state has a polynomial tail $t^{-\beta}$, we expect the decay rate of correlation to be also $\sim t^{-\beta}$. Although a rigorous proof for the billiard model is difficult, this approach can be rigorously justified for simpler deterministic dynamical systems and Markov chains. We refer readers to [19] for the induced chain method for Markov processes and [29, 30] for the Young towers of deterministic dynamical systems.

In Figure 4.5, we showed the tail of the first passage time to the high energy state

$$A = \{(\mathbf{x}_1^1, \mathbf{v}_1^1, \mathbf{x}_2^1, \mathbf{v}_2^1), (\mathbf{x}_1^2, \mathbf{v}_1^2, \mathbf{x}_2^2, \mathbf{v}_2^2) \mid |\mathbf{v}_1^i|^2 + |\mathbf{v}_2^i|^2 \geq 0.2, i = 1, 2\} \subset \Omega$$

for a 2-cell 4-particle model. The total kinetic energy in the system is set to be 1. Since the rate $\sqrt{\min\{E_i, E_{i+1}\}}$ only occurs when one of the total cell energy is sufficiently small (less than 0.01 in our case), we need some importance sampling to reduce the computational cost. The initial cell total cell energy is sampled from the distribution of post-collision total cell energy, conditioning with the event that the left cell energy is less than 0.001. We can see that the tail of first passage time to the high energy set is $\sim t^{-4}$. This supports our claim that the decay rate of correlation should be t^{-2M} .

5. COMPARISON OF THERMAL CONDUCTIVITY

It remains to compare the thermal conductivity of the billiard model and that of the stochastic energy exchange model. It has been reported in [11] that the billiard model has a “normal” thermal conductivity, i.e., the thermal conductivity is proportional to the reciprocal of the length of the chain. We use Monte Carlo simulations to verify that the stochastic energy exchange model also has the “normal” thermal conductivity.

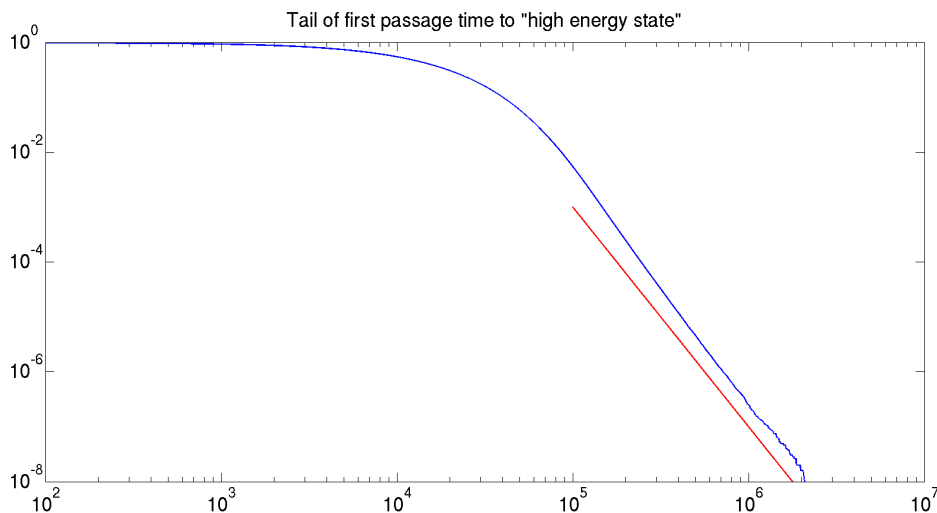


FIGURE 14. Blue: Tail of first passage time $\mathbb{P}[\tau_A > t]$. Red: reference line with slope -4 .

We define the empirical thermal conductivity in the following way. Consider a stochastic energy exchange model with N sites and boundary temperatures T_L and T_R . We take the convention that site 0 and $N + 1$ are the left and the right heat baths respectively. Let $J(t_i, k)$ be the energy flux from right to left if one energy exchange occurs between site k and site $k + 1$ at time t_i . More precisely, we have

$$J(t_i, k) = \begin{cases} E'_k - E_k & \text{if } k \neq 0 \\ E_{k+1} - E'_{k+1} & \text{if } k = 0, \end{cases}$$

if E_k and E_{k+1} exchanges energy at t_i . When starting from the invariant probability measure π , the *thermal conductivity* is defined as

$$\kappa = \lim_{T \rightarrow \infty} \frac{1}{T} \frac{1}{T_R - T_L} \sum_{t_i < T} J(t_i, k).$$

In the numerical simulation, we fix boundary temperatures as $T_L = 1$ and $T_R = 2$. The thermal conductivity is then computed for increasing N , as shown in Figure 15. The least square curve fitting gives a linear relation

$$\kappa(N) = \frac{0.0752}{N} + 4.02 \times 10^{-5}.$$

We believe this numerical result confirms that κ is proportional to $1/N$.

6. CONCLUSION

In this paper we studied a nonequilibrium billiard model that mimics the dynamics of gas particles in a long and thin tube. Due to the significant difficulty of working on the deterministic system directly, we carry out a series of numerical simulations to study the rule of energy exchanges between cells, which is essentially given by the collision event that involves particles from neighboring cells. The time distribution

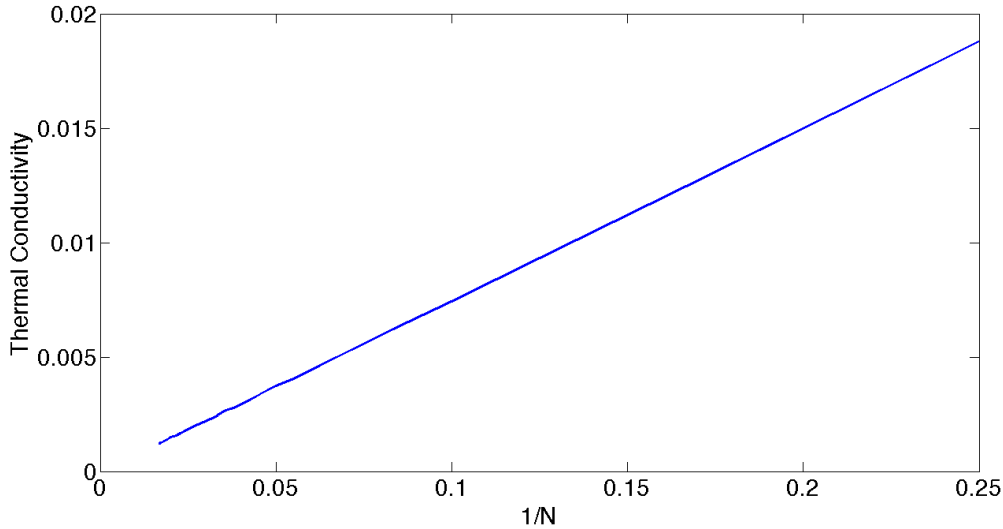


FIGURE 15. Thermal conductivity for increasing N from 4 to 60. Thermal conductivity is computed through long time averaging up to $T = 60000$ of 80 samples.

of such events and the post-collision energy distribution are studied. Numerical results show the time evolution of the energy profile of the deterministic system is approximated by a much simpler stochastic energy exchange model.

We then use a computer assisted method proposed in [20] to compare the stochastic energy exchange model and the original billiard system. The conclusion is that the key dynamical properties of the billiard model is preserved by the stochastic energy exchange model. Both of them has polynomial ergodicity. The speed of correlation decay are both $O(t^{-2M})$, where M is the number of particles in a cell. The thermal conductivity of both models are proportional to $1/N$.

This result opens the door of many further investigations, as the stochastic energy exchange model is tractable for many rigorous studies. For example, the polynomial ergodicity can be rigorously proved by using the same technique developed in [19]. In addition to the ergodicity, the mesoscopic limit problem is also worth to study. When the number of particles in a cell is large, each collision will only exchange a small amount of energy. Hence the stochastic energy exchange model (after a time rescaling) has interesting slow-fast dynamics. Such slow-fast dynamics can be approximated by a stochastic differential equation (the mesoscopic limit equation). Many macroscopic thermodynamic properties can be further derived from the mesoscopic limit equation.

This paper serves as the first paper of a sequel that aims to connect billiards-like deterministic dynamics and macroscopic thermodynamic laws. We will write separate papers to address the ergodicity, mesoscopic limit, and macroscopic properties of the stochastic energy exchange model.

REFERENCES

- [1] F. Bonetto, J.L. Lebowitz, and L. Rey-Bellet, *Fourier's law: a challenge to theorists*, Mathematical physics 2000 (2000), 128–150.
- [2] Leonid Bunimovich, Carlangelo Liverani, Alessandro Pellegrinotti, and Yurii Suhov, *Ergodic systems of n balls in a billiard table*, Communications in mathematical physics **146** (1992), no. 2, 357–396.
- [3] Leonid A Bunimovich, D Burago, N Chernov, EGD Cohen, CP Dettmann, JR Dorfman, S Ferleger, R Hirschl, A Kononenko, JL Lebowitz, et al., *Hard ball systems and the lorentz gas*, vol. 101, Springer Science & Business Media, 2013.
- [4] Leonid A Bunimovich and Ya G Sinai, *Statistical properties of lorentz gas with periodic configuration of scatterers*, Communications in Mathematical Physics **78** (1981), no. 4, 479–497.
- [5] Leonid Abramovich Bunimovich, Yakov Grigor'evich Sinai, and Nikolai Ivanovich Chernov, *Statistical properties of two-dimensional hyperbolic billiards*, Russian Mathematical Surveys **46** (1991), no. 4, 47–106.
- [6] Nikolai Chernov and Lai-Sang Young, *Decay of correlations for lorentz gases and hard balls*, Hard ball systems and the Lorentz gas, Springer, 2000, pp. 89–120.
- [7] Nikolai Chernov and Hong-Kun Zhang, *Billiards with polynomial mixing rates*, Nonlinearity **18** (2005), no. 4, 1527.
- [8] Bernard Derrida, *An exactly soluble non-equilibrium system: the asymmetric simple exclusion process*, Physics Reports **301** (1998), no. 1, 65–83.
- [9] Jean-Pierre Eckmann, Claude-Alain Pillet, and Luc Rey-Bellet, *Entropy production in non-linear, thermally driven hamiltonian systems*, Journal of statistical physics **95** (1999), no. 1-2, 305–331.
- [10] J.P. Eckmann and L.S. Young, *Nonequilibrium energy profiles for a class of 1-d models*, Communications in mathematical physics **262** (2006), no. 1, 237–267.
- [11] Pierre Gaspard and Thomas Gilbert, *Heat conduction and fourier's law in a class of many particle dispersing billiards*, New Journal of Physics **10** (2008), no. 10, 103004.
- [12] ———, *Heat conduction and fouriers law by consecutive local mixing and thermalization*, Physical review letters **101** (2008), no. 2, 020601.
- [13] ———, *On the derivation of fourier's law in stochastic energy exchange systems*, Journal of Statistical Mechanics: Theory and Experiment **2008** (2008), no. 11, P11021.
- [14] A. Grigo, K. Khanin, and D. Szasz, *Mixing rates of particle systems with energy exchange*, Nonlinearity **25** (2012), no. 8, 2349.
- [15] N Haydn, Y Lacroix, S Vaienti, et al., *Hitting and return times in ergodic dynamical systems*, The annals of Probability **33** (2005), no. 5, 2043–2050.
- [16] Nicolai Haydn and Sandro Vaienti, *The compound poisson distribution and return times in dynamical systems*, Probability theory and related fields **144** (2009), no. 3, 517–542.
- [17] C. Kipnis, C. Marchioro, and E. Presutti, *Heat flow in an exactly solvable model*, Journal of Statistical Physics **27** (1982), no. 1, 65–74.
- [18] Yao Li, *On the stochastic behaviors of locally confined particle systems*, Chaos: An Interdisciplinary Journal of Nonlinear Science **25** (2015), no. 7, 073121.
- [19] ———, *On the polynomial convergence rate to nonequilibrium steady-states*, arXiv preprint arXiv:1607.08492 (2016).
- [20] Yao Li and Hui Xu, *Numerical simulation of polynomial-speed convergence phenomenon*, Journal of Statistical Physics **169** (2017), no. 4, 697–729.
- [21] Yao Li and Lai-Sang Young, *Existence of nonequilibrium steady state for a simple model of heat conduction*, Journal of Statistical Physics **152** (2013), no. 6, 1170–1193.
- [22] ———, *Nonequilibrium steady states for a class of particle systems*, Nonlinearity **27** (2014), no. 3, 607.
- [23] Yao Li, Lai-Sang Young, et al., *Polynomial convergence to equilibrium for a system of interacting particles*, The Annals of Applied Probability **27** (2017), no. 1, 65–90.

- [24] C. Liverani, S. Olla, et al., *Toward the fourier law for a weakly interacting anharmonic crystal*, Journal of the American Mathematical Society **25** (2011), 555–583.
- [25] Luc Rey-Bellet and L Thomas, *Exponential convergence to non-equilibrium stationary states in classical statistical mechanics*, Communications in mathematical physics **255** (2001), no. 2, 305–329.
- [26] Luc Rey-Bellet and Lawrence E Thomas, *Fluctuations of the entropy production in anharmonic chains*, Annales Henri Poincare, vol. 3, Springer, 2002, pp. 483–502.
- [27] Nándor Simányi, *Proof of the boltzmann-sinai ergodic hypothesis for typical hard disk systems*, Inventiones Mathematicae **154** (2003), no. 1, 123–178.
- [28] Nándor Simányi and Domokos Szász, *Hard ball systems are completely hyperbolic*, Annals of Mathematics **149** (1999), 35–96.
- [29] Lai-Sang Young, *Statistical properties of dynamical systems with some hyperbolicity*, Annals of Mathematics (1998), 585–650.
- [30] ———, *Recurrence times and rates of mixing*, Israel Journal of Mathematics **110** (1999), no. 1, 153–188.

YAO LI: DEPARTMENT OF MATHEMATICS AND STATISTICS, UNIVERSITY OF MASSACHUSETTS AMHERST, USA

E-mail address: yaoli@math.umass.edu

LINGCHEN BU: DEPARTMENT OF MATHEMATICS AND STATISTICS, UNIVERSITY OF MASSACHUSETTS AMHERST, USA

E-mail address: lingchen.l.bu@gmail.com